Bioorganic Chemistry 111 (2021) 104885

Contents lists available at ScienceDirect

Bioorganic Chemistry

journal homepage: www.elsevier.com/locate/bioorg

Novel 1,2,4-oxadiazole-chalcone/oxime hybrids as potential antibacterial DNA gyrase inhibitors: Design, synthesis, ADMET prediction and molecular docking study

Tarek S. Ibrahim [a,b,*], Ahmad J. Almalki [a], Amr H. Moustafa [c], Rasha M. Allam [d], Gamal El-Din A. Abuo-Rahma [e,f], Hussein I. El Subbagh [g], Mamdouh F.A. Mohamed [h,*]

[a] Department of Pharmaceutical Chemistry, Faculty of Pharmacy, King Abdulaziz University, Jeddah 21589, Saudi Arabia
[b] Department of Pharmaceutical Organic Chemistry, Faculty of Pharmacy, Zagazig University, Zagazig 44519, Egypt
[c] Department of Chemistry, Faculty of Science, Sohag University, Sohag 82524, Egypt
[d] Pharmacology Department, National Research Centre, Cairo 12622 (ID: 60014618), Egypt
[e] Department of Medicinal Chemistry, Faculty of Pharmacy, Minia University, Minia 61519, Egypt
[f] Department of Pharmaceutical Chemistry, Faculty of Pharmacy, Deraya University, New Minia, Minia, Egypt
[g] Department of Medicinal Chemistry, Faculty of Pharmacy, Mansoura University, 35516 Mansoura, Egypt
[h] Department of Pharmaceutical Chemistry, Faculty of Pharmacy, Sohag University, 82524 Sohag, Egypt

ARTICLE INFO

Keywords:
Chalcone
1,2,4-Oxadiazole
Antibacterial
DNA gyrase
ADMET
Docking studies

ABSTRACT

New antibacterial drugs are urgently needed to tackle the rapid rise in multi-drug resistant bacteria. DNA gyrase is a validated target for the development of new antibacterial drugs. Thus, in the present investigation, a novel series of 1,2,4-oxadiazole-chalcone/oxime (**6a-f**) and (**7a-f**) were synthesized and characterized by IR, NMR (^{1}H and ^{13}C) and elemental analyses. The title compounds were evaluated for their *in-vitro* antimicrobial activity by the modified agar diffusion method as well as their *E. coli* DNA gyrase inhibitory activity. The minimum inhibitory concentration (MIC) and the structure activity relationships (SARs) were evaluated. Among all, compounds **6a**, **6c-e**, **7b** and **7e** were the most potent and proved to possess broad spectrum activity against the tested Gram-positive and Gram-negative organisms. Additionally, compounds **6a** (against *S. aureus)*, **6c** (against *B. subtilis* and *E. hirae*), **6e** (against *E. hirae*), **6f**, **7a** and **7c** (against *E. coli)* and **7d** (against *B. subtilis)*, with MIC value of 3.12 μM were two-fold more potent than the standard ciprofloxacin (MIC = 6.25 μM). Mechanistically, compounds **6c**, **7c**, **7e** and **7b** had good inhibitory activity against *E. coli* gyrase with IC_{50} values of 17.05, 13.4, 16.9, and 19.6 μM, respectively, in comparison with novobiocin (IC_{50} = 12.3 μM) and ciprofloxacin (IC_{50} = 10.5 μM). The molecular docking results at DNA gyrase active site revealed that the most potent compounds **6c** and **7c** have binding mode and docking scores comparable to that of ciprofloxacin and novobiocin suggesting their antibacterial activity *via* inhibition of DNA gyrase. Finally, the predicted parameters of Lipinski's rule of five and ADMET analysis showed that **6c** and **7c** had good drug-likeness and acceptable physicochemical properties. Therefore, the hybridization of the chalcone and oxadiazole moieties could be promising lead as antibacterial candidate which merit further future structural optimizations.

1. Introduction

The treatment of infectious diseases remains as a vital and challenging problem due to the rapid rise in multi-drug resistant microorganisms and the limited number of efficacious antimicrobial drugs [1]. Despite the availability of a large number of chemotherapeutics and antibiotics, the appearance of antibiotic resistant bacterial strains represent a substantial need for the synthesis and the discovery of new safer and potent antimicrobial agents [2]. Interrupting the replication of DNA represents an effective and a promising antibacterial mechanism [3]. DNA gyrase is classified as type II topoisomerase that is involved in maintenance of the correct spatial of DNA topology in bacteria and it is

* Corresponding authors at: Department of Pharmaceutical Chemistry, Faculty of Pharmacy, King Abdulaziz University, Jeddah 21589, Saudi Arabia (T.S. Ibrahim).
E-mail addresses: tmabrahem@kau.edu.sa (T.S. Ibrahim), mamdouh.fawzi@pharm.sohag.edu.eg (M.F.A. Mohamed).

https://doi.org/10.1016/j.bioorg.2021.104885
Received 31 January 2021; Received in revised form 26 March 2021; Accepted 28 March 2021
Available online 1 April 2021

independently crucial for bacterial DNA replication [4,5]. DNA gyrase includes two copies of GyrA (which contains the catalytic tyrosine) and two copies of GyrB (which comprises the ATPase activity) [6]. DNA gyrase has a vital role in all bacteria except higher eukaryotes as it is absent in humans and this makes it an attractive and validated therapeutic target for development of new antibacterial agents for decades, being the target of fluoroquinolones antibiotics [7]. As the currently used drugs have undesirable side effects and have the abilities in developing rapid resistance, the discovery of more potent and effective antimicrobial agents is strongly recommended.

Although chalcones have no structural or pharmacodynamic similarities with the broad-spectrum antibiotics, they have been identified to be such alternative. Chalcones and their derivatives gained a great attention due to their diverse and interesting biological activities [8] such as analgesic [9] anti-inflammatory [10], antimalarial [11,12], antioxidant [13,14], antifungal [15,16], anti-tuberculosis [17], antibacterial (Fig. 1, compounds **I** and **II**) [18], parasitic protease inhibitors [19], antiviral [20], anti-human immunodeficiency virus (HIV) [21], HDAC inhibitors [22], antitumor activities [23,24] and as insulin mimetic in 3 T3-L1 adipocyte [25]. Moreover, many chalcone derivatives exhibited good antimicrobial activity *via* inhibition of DNA gyrase such as compounds **III-VI** [26] (Fig. 1).

On the other hand, the five membered heterocyclic 1,2,4-oxadizole scaffold has been widely utilized as a core unit in a diversity of bioactive molecules displaying diverse biological activities such as anti-inflammatory, anticonvulsant, anticancer, anxiolytic, antidepressant,

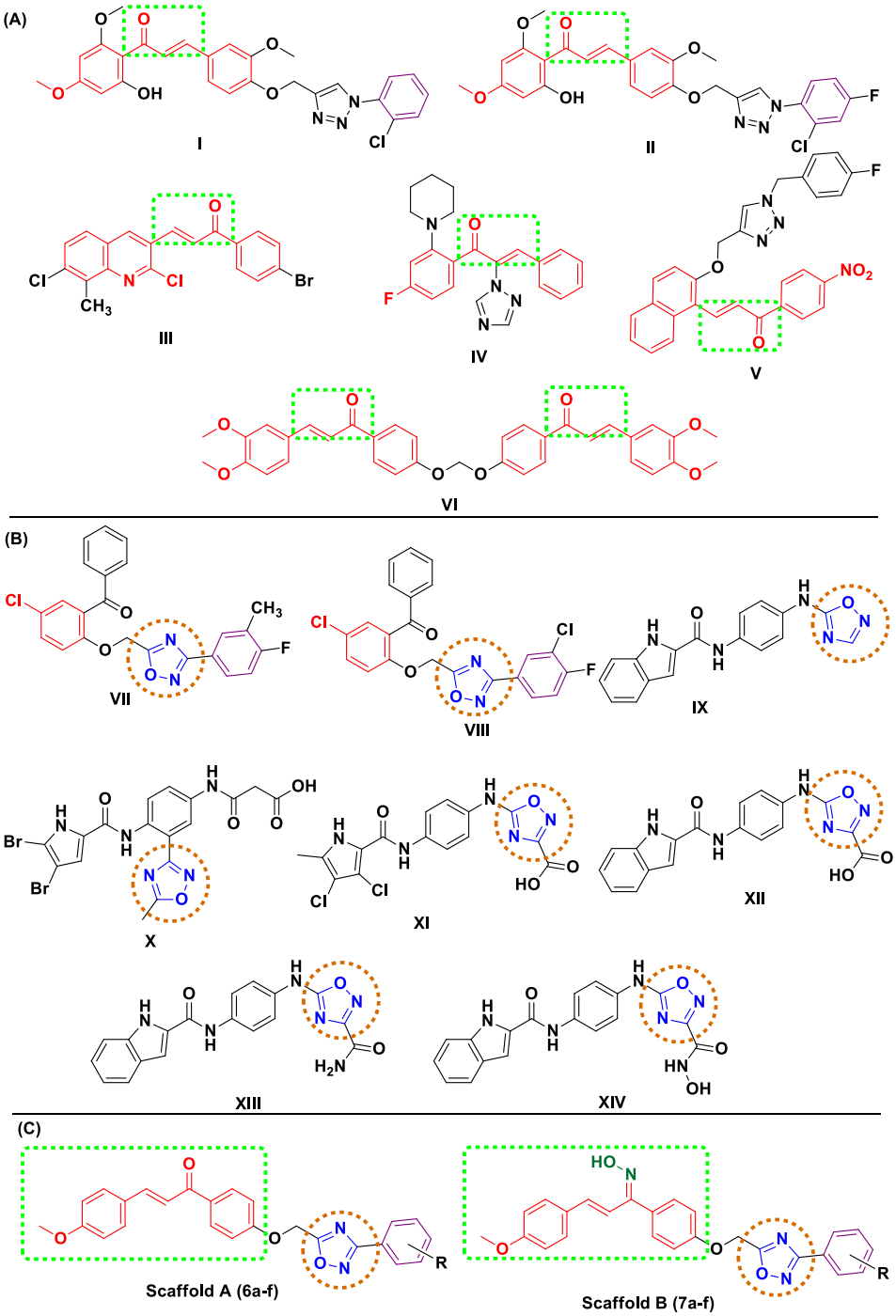

Fig. 1. Representative examples antibacterial chalcones (A), oxadiazole derivatives (B) and the target 1,2,4-oxadiazole-chalcone/oxime hybrids (**6a-f** and **7a-f**) (C).

analgesic, antiparasitic, antifungal [27] and antimicrobial such as compounds **VII** and **VIII** [28], antibacterial *via* inhibition of DNA gyrase (Fig. 1, compounds **IX-XIV**) [29–31]. Moreover, it was proved that 1,2,4-oxadizole-containing compounds show inhibitory potency against Penicillin-Binding Protein (PBP2a), cyclooxygenase (COX-1 and COX-2), Human Deacetylase Sirtuin 2 (HDSirt2), Histone Deacetylase (HDAC), Carbonic Anhydrase (CA), dual COX-2/15-LOX inhibitors and dual iNOS/PGE2 inhibitors [27,32,33]. In addition, 1,2,4-oxadiazole scaffold has emerged an acceptable pharmacokinetic profile; this recommend it to be used in the "hit-to-lead" optimization in drug discovery [33]. Importantly, 1,2,4-oxadiazole exhibited rigid equivalence to amide and ester functional groups due to creation of specific interaction such as hydrogen bonding and/or when the instability of those groups is noticed due to factors like hydrolysis [32].

Molecular hybridization in which two pharmacophoric moieties are combined in a one single molecule with additive biological properties is a promising approach in drug design and development. This strategy aims to innovate new hybrids with the potential not only to improve affinity and efficacy but also to overcome cross resistance compared with the parent drugs and can result in modified selectivity profile and/or dual modes of action with reduced undesirable side effects [34]. Therefore, encouraged and motivated by the known antibacterial importance of both chalcones and 1,2,4-oxadiazole moieties, this research study aims at the first-in-class synthesis of novel 1,2,4-oxadiazole-chalcone/oxime hybrids (Fig. 1). Meanwhile, the antimicrobial evaluation of the target compounds was done using a panel of Gram-positive, Gram-negative and fungal strains. Moreover, the DNA-gyrase inhibition assay is reported and molecular docking into DNA gyrase protein pocket (PDB ID: 4DUH) is carried out to investigate the binding affinity and binding mode of the most active compounds.

2. Results and discussion

2.1. Chemistry

The synthetic approach to obtain the target 1,2,4-oxadiazole-chalcone/oxime (**6a-f**) and (**7a-f**) is described in Scheme 1. The key chalcone acid **3** [22], cyano derivatives **4a-f** and amidoximes **5a-f** were produced according to the reported procedures as described in the literature [32,33,35].

1,2,4-Oxadiazole-chalcone derivatives **6a-f** were formed *via* reaction of the acetic acid derivative **3** with amidoximes **5a-f**, using *N,N′*-carbonyldiimidazole (CDI) and heating under reflux. The structural formula of 3-aryl-1,2,4-oxadiazole-chalcone hybrids **6a-f** were elucidated by IR, ^{1}H NMR, ^{13}C NMR spectra and elemental analyses. The ^{1}H NMR spectrum of **6b** exhibited the appearance of two singlet signals at δ 3.83 and 5.76 ppm which were assigned to methoxy and methylene protons, respectively. The aromatic protons and ^{13}C NMR signals appeared at their expected chemical shift. (*see* **Supporting Information**). Condensation of 3-aryl-1,2,4-oxadiazoles **6a-f** with hydroxylamine hydrochloride afforded the keto-oxime derivatives **7a-f**. The structure of oximes **7a-f** was elucidated based on IR, ^{1}H NMR, ^{13}C NMR spectra and elemental analyses. IR spectrum of **7b** exhibited the appearance of the new characteristic broad band at 3263 cm^{-1} due to O—H, and disappearance of characteristic absorption band at 1652 cm^{-1} for carbonyl group. The ^{1}H NMR spectrum of **7b** revealed the appearance of the new singlet signal at δ 11.36 ppm which is attributed to the oximic OH group; in addition to other signals in aliphatic and aromatic regions. Also, ^{13}C NMR and elemental analyses confirms the structure (*see* **Supporting Information**). The configuration of the double bond of chalcone moiety could be confirmed by the ^{1}H NMR spectrum. For example, chalcone **7d** showed an olefinic proton H-β as singlet at 5.63 ppm and the other as doublet at 6.68 ppm with high *J* coupling constant of 16.4 Hz attributed to H-α of chalcone double bond. Thus, both protons are magnetically inequivalent besides high *J* coupling constant support the characteristic *E*-configuration of the synthesized chalcones [8,36,37]. Furthermore, the ^{13}C NMR spectrum of compound **7f**, as a representative example, characterized by the presence of downfield signals corresponding to the carbons of α,β-unsaturated system represented at 116.0 and 136.9 ppm evidencing the (*E*)-configuration of the synthesized chalcones [38,39].

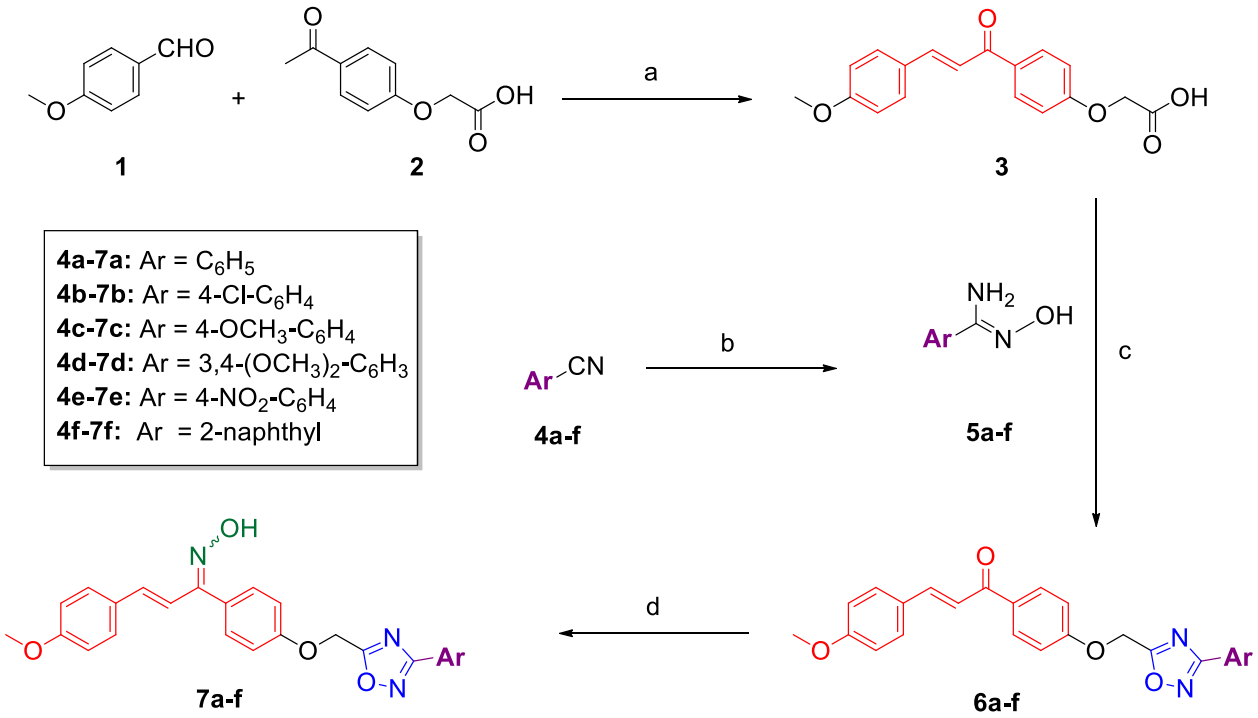

Scheme 1. Synthesis of target compounds **6a-f** and **7a-f**. **Reagents and conditions**: (a) 10% NaOH, EtOH, then HCl; (b) $NH_2OH.HCl$, K_2CO_3, MeOH, reflux; 5–8 h; (c) CDI, CH_3CN, reflux, 24 h; (d) $NH_2OH.HCl$, pyridine, CDI, 60° C, 4 h, then HCl.

2.2. Biology evaluation

2.2.1. Antimicrobial activity

The synthesized 1,2,4-oxadiazole-chalcone/oxime (**6a-f**) and (**7a-f**), were screened for their antimicrobial activity against panel of Gram-positive bacteria (*Bacillus subtilis*, *Staphylococcus aureus*, *Enterococcus hirae)*, Gram-negative bacteria (*Pseudomonas aeruginosa*, *Klebsiella pneumonia*, *Escherichia coli*) and yeast (*C. albicans*). Sulfamethoxazole, Ciprofloxacin and Clotrimazole were used as antibacterial and antifungal standards, respectively. Results are showed in Table 1, as minimal inhibitory concentrations (MICs).

The antibacterial results against *E. hirae* showed that all 1,2,4-oxadiazole/oxime hybrids **7a-f**, except for **7d**, revealed good antimicrobial activity with MIC value 6.25 similar to ciprofloxacin and sulfamethoxazole (MIC = 6.25 μM). Among 1,2,4-oxadiazole/chalcone hybrids **6a-f**, hybrids **6c** and **6e** showed the best potential MIC value (3.21 μM) with two-fold higher in activity than ciprofloxacin and sulfamethoxazole. Compound **6b** with MIC = 6.25 μM showed equal potency to ciprofloxacin. Compounds **6d** and **6f** (MIC = 12.5 μM) showed moderate antibacterial activity whereas compound **6a** was the least active compound against *E. hirae* (MIC = 25 μM). Regarding *S. aureus*, Compound **6a** proved the highest activity with a MIC value of 3.12 μM, which was two-fold more potent than ciprofloxacin (*S. aureus* MIC = 6.25 μM) and four-fold higher than sulfamethoxazole (*S. aureus* MIC = 12.5 μM). Compound **7d** showed similar antimicrobial activity as ciprofloxacin. Where compounds **6c**, **6e**, **7c**, **7e**, **7f** exhibited comparable antibacterial activity compared to sulfamethoxazole but with lower activity than ciprofloxacin. Compounds **6d**, **7a**, **7b** displayed weaker antibacterial activity compared to the used standards. Finally, compounds **6b** and **6f** were devoid of any bacterial activity. Concerning *B. subtilis*, compounds **6c** and **7d** (MIC = 3.12) were the most potent and displayed two-fold higher in activity than ciprofloxacin (MIC = 6.25). Compounds **6a**, **6d**, **6f** and **7f** showed good activity while the remaining derivatives demonstrated moderate potencies in comparison with the reference drugs.

E. coli was one of the highly sensitive Gram-negative bacteria for the tested compounds. Compounds (**6f**, **7a**, **7c**) and (**6c**, **7b**, **7e**, **7f**) displayed equipotent antibacterial activity against *E. coli* with MIC of 3.12 and 6.25 μM, respectively, and of almost four and two-fold higher activity than Sulfamethoxazole (MIC = 12.5 μM). The remaining compounds except for **6e** demonstrated similar potencies in comparison with sulfamethoxazole and with lower potencies compared to ciprofloxacin (MIC = 6.25 μM). Additionally, the promising activity against *P. aeruginosa* was observed from all compounds except compound **6f**. However, *K. pneumoniae* was the most resistant Gram-negative bacteria. It was noticed that only **6e** and **6f** yielded similar MIC value (6.25 μM) to ciprofloxacin and sulfamethoxazole. The antifungal effectiveness against C. albicans ranged from weak to no effect at all for all tested compounds. Compounds **6f** and **7e** showed potencies against *C. albicans* with MIC value of 25 μM.

2.2.2. Inhibition of DNA-Gyrase supercoiling activity

The observed antimicrobial activity (MIC values) of the tested compounds against *E. coli* inspired the assessment of their potential anti-gyrase activity. The reference drugs that targeting DNA gyrase by the two main mechanisms were used: Ciprofloxacin (the inhibitor of GyrA active site DNA complex) and Novobiocin (the inhibitor of GyrB subunit ATPase function) [40,41].

Regarding 1,2,4-oxadiazole/oxime hybrids, compounds **7c**, **7e** and **7b** exhibited good inhibitory activity against *E. coli* gyrase with IC_{50} values of 13.4 μM, 16.9 μM, and 19.6 μM, respectively in comparison with Novobiocin (IC_{50} = 12.3 μM) and ciprofloxacin (IC_{50} = 10.5 μM). While hybrids **7a**, **7d**, and **7f** displayed low inhibitory activity against *E. coli* gyrase with IC_{50} values of 35.5 μM, 23.6 μM, 30.5 μM, respectively. Concerning, 1,2,4-oxadiazole/chalcone hybrids, in general, all compounds **6a-f** showed moderate inhibition of *E. coli* gyrase with IC_{50} range from 29.6 μM to 44.9 μM except for **6c** that showed good *E. coli* gyrase inhibition with IC_{50} of 17.05 μM. The IC_{50} values are listed in Table 2 and demonstrated in Fig. 2. From these results, it is obvious that compounds **7c** and **6c** were the most active compounds among their series with IC_{50} values of 13.49 and 17.05 μM, respectively.

2.2.3. Cell viability assay

Cell viability assay was carried out using human mammary gland epithelial cell line (MCF-10A) [42]. Compounds **6c** and **7c** have been incubated with MCF-10A cells for 96 h and 3-(4,5-dimethylthiazol-2-yl)-2,5-diphenyltetrazolium bromide (MTT) assay was used to determine

Table 2
Inhibition of DNA-Gyrase supercoiling activity of compounds **6a-f** and **7a-f.**

***E. coli* DNA-gyrase inhibition**			
Compound No.	**IC_{50} (μM)**	**Compound No.**	**IC_{50} (μM)**
6a	44.95 ± 2.56	**7a**	35.55 ± 2.02
6b	40.66 ± 2.32	**7b**	19.65 ± 1.12
6c	17.05 ± 0.97	**7c**	13.49 ± 0.77
6d	33.57 ± 1.91	**7d**	23.7 ± 1.35
6e	38.95 ± 2.22	**7e**	16.99 ± 0.97
6f	29.62 ± 1.69	**7f**	30.53 ± 1.74
Ciprofloxacin	10.5 ± 0.6	**Novobiocin**	12.36 ± 0.7

Table 1
MIC values of tested compounds **6a-f** and **7a-f** against Gram-positive, Gram-negative organisms and fungi.

Minimal Inhibitory Concentration (MIC) in μM							
Compound No.	**Gram-positive organisms**			**Gram-negative organisms**			Fungi
	B. subtilis	***E. hirae***	***S. aureus***	***E. coli***	***K. pneumoniae***	***P. aeruginosa***	*C. albicans*
6a	6.25	25	3.12	12.5	25	12.5	na
6b	12.5	6.25	na	12.5	na	12.5	na
6c	3.12	3.12	12.5	6.25	50	6.25	na
6d	6.25	12.5	50	12.5	12.5	6.25	na
6e	12.5	3.12	12.5	25	6.25	12.5	na
6f	6.25	12.5	na	3.12	6.25	25	25
7a	12.5	6.25	25	3.12	na	12.5	na
7b	12.5	6.25	25	6.25	12.5	6.25	na
7c	na	6.25	12.5	3.12	na	12.5	na
7d	3.12	25	6.25	12.5	na	12.5	na
7e	12.5	6.25	12.5	6.25	25	6.25	25
7f	6.25	6.25	12.5	6.25	na	6.25	na
Sulfamethoxazole	6.25	6.25	12.5	12.5	6.25	12.5	nd
Ciprofloxacin	6.25	6.25	6.25	6.25	6.25	6.25	nd
Clotrimazole	nd	nd	nd	nd	nd	nd	12.5

na, not active; nd, not determined

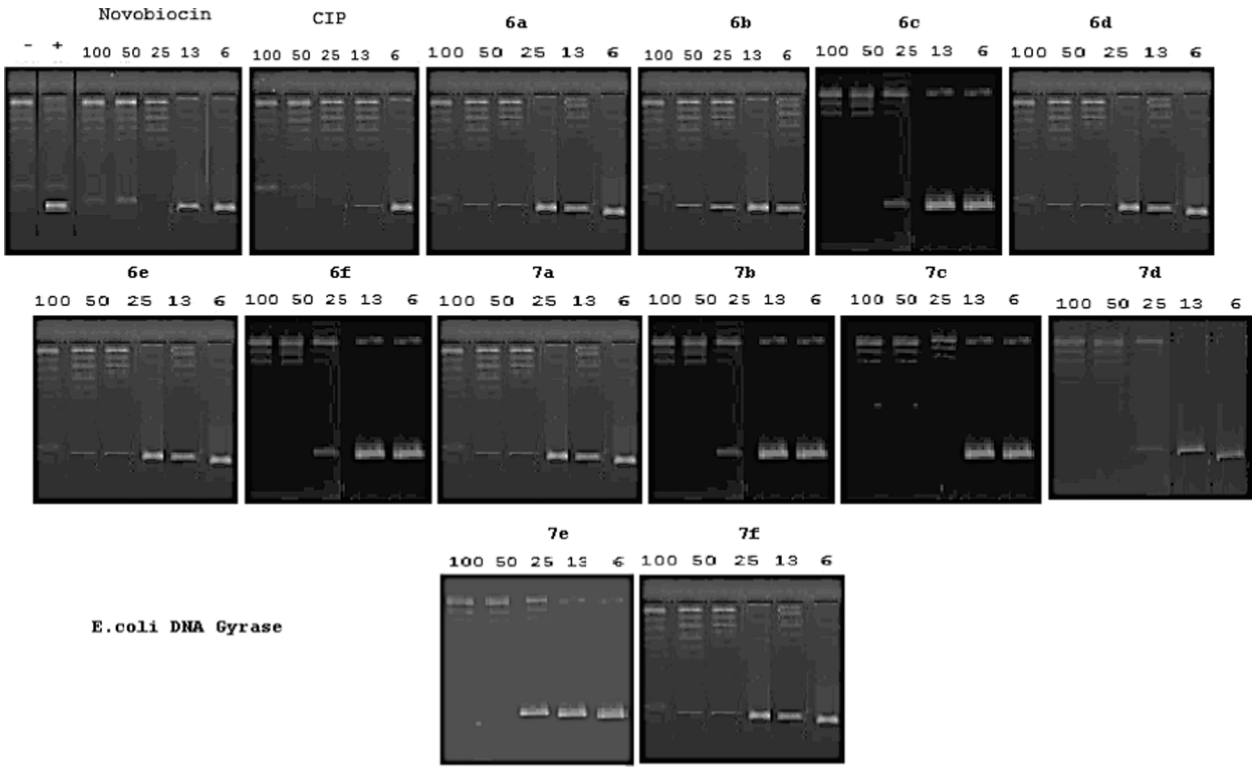

Fig. 2. Agarose gel electrophoresis of E-coli DNA gyrase supercoiling activity of compounds **6a-f** and **7a-f**, novobiocin and ciprofloxacin using a microplate assay kit (Inspiralis). 1U of DNA gyrase is incubated with 0.5 μg of relaxed pBR322 in a reaction volume of 30 μl at 37 °C for 30 min in Assay Buffer. Negatively supercoiled plasmids form intermolecular triplex DNA more readily than do relaxed plasmids. Gels are run in the absence of ethidium bromide or chloroquine.

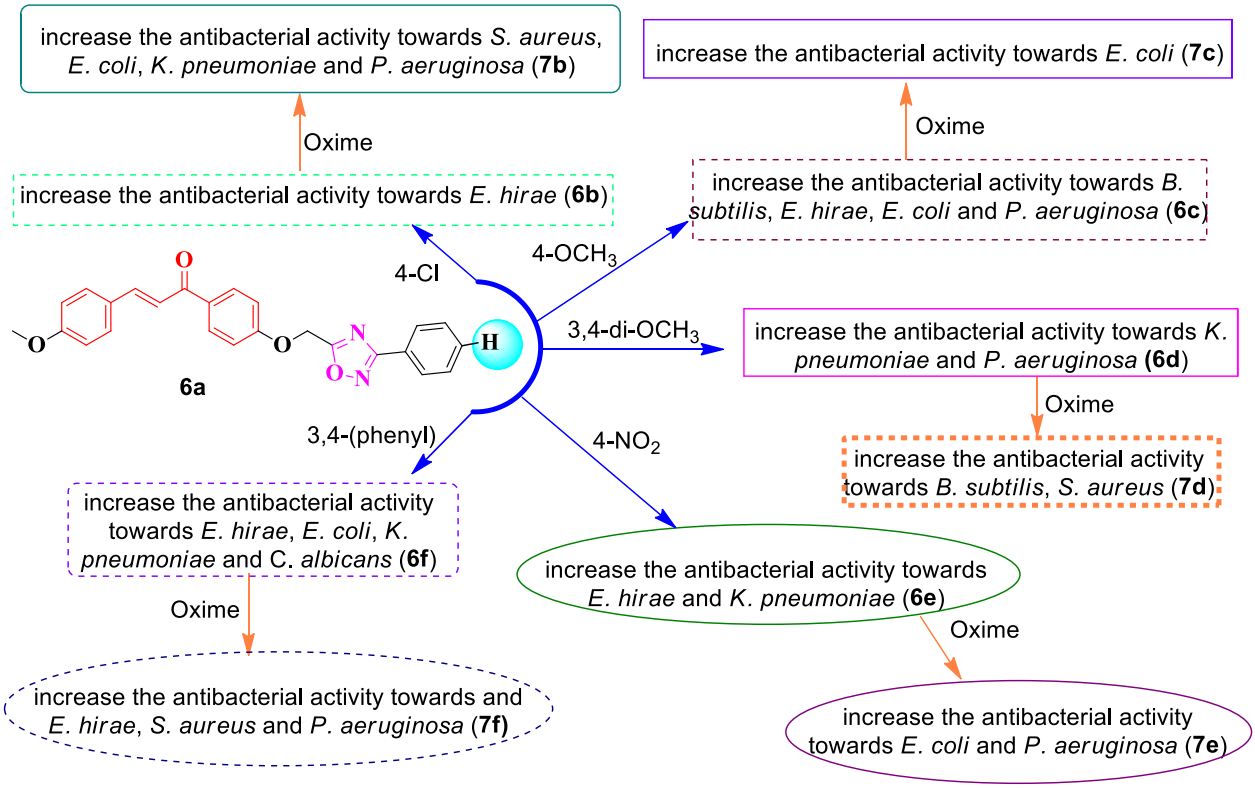

Fig. 3. SAR of the synthesized target compounds **6a-f** and **7a-f**.

the cell viability. Both compounds showed no cytotoxic effects and the viability of the cells for the tested compounds was 93% and 89% for compound **6c** and **7c**, respectively, at 50 μM.

2.3. Structure activity relationship (SAR)

A novel series of compounds namely: 1,2,4-oxadiazole/chalcone hybrids **6a-f** and 1,2,4-oxadiazole/oxime hybrids **7a-f**, were synthesized and tested for their antimicrobial activities (Tables 1), in addition to DNA-Gyrase supercoiling inhibitory activity (Table 2, **Figures** and **2**). In general, there is no significant difference in potency between the 1,2,4-oxadiazole/chalcone hybrids (**6a-f**) and 1,2,4-oxadiazole/oxime hybrids (**7a-f**) in potency. Moreover, the active compounds in both series have a broad-spectrum activity against the tested Gram-positive and Gram-negative strains. Concerning the 1,2,4-oxadiazole/chalcone hybrids, substituent at the 3-phenyl-oxadiazole moiety proved to have a significant role in activity. Compounds **6a** (unsubstituted-phenyl) and **6c** (4-OCH_3-phenyl) showed a broad-spectrum antibacterial potency. The introduction of 3,4-dimethoxy-phenyl (**6d**), electron withdrawing chlorine (**6b**) or nitro function (**6e**) decreased the magnitude of activity. The structure activity relationship (Fig. 3) can be summarized as follows: Replacement of hydrogen atom with the electron withdrawing Cl atom as in compound **6b**, resulted in increase the antibacterial activity towards *E. hirae*, while retain the same activity against *E. coli* and P. aeruginosa. Conversion of chalcone **6b** into its oxime counterpart yielded compound **7b** with increased antibacterial activity towards *S. aureus, E. coli, K. pneumoniae and P. aeruginosa.* Introducing the donating group OCH_3 (**6c**) increases the antibacterial activity towards *B. subtilis*, *E. hirae*, *E. coli* and *P. aeruginosa* where its oxime derivatives **7c** lead to increase the antibacterial activity towards *E. coli.* Increases the electron donation by adding 3,4-di-OCH_3 as in chalcone **6d** increases the antibacterial activity towards *K. pneumoniae* and *P. aeruginosa*, while its oxime **7d** increases the antibacterial activity towards *B. subtilis* and *S. aureus*. Introducing the strongly deactivating NO_2 group as in **6e** increases the antibacterial activity towards *E. hirae*, *K.* and *pneumoniae* while its oxime **7e** increases the antibacterial activity towards *E. coli* and *P. aeruginosa*. Replacement of the phenyl group with the bulky 2-naphthyl group as in **6f** lead to increase the antibacterial activity towards *E. hirae*, *E. coli*, *K. pneumoniae* and *C. albicans*, while its oxime counterpart **7f** increases the antibacterial activity towards *E. hirae*, *S. aureus* and *P. aeruginosa.*

2.4. Molecular modeling and docking study

Discovery Studio 2.5 software was used to investigate the binbing ability of compounds **6c**, **7c** along with ciprofloxacin and novobiocin into the active site of *E. coli* DNA gyrase protein. The 3D co-crystal structure (PDB ID: 4DUH) with benzimidazol-2-ylurea inhibitor was downloaded from the Protein Data Bank. The virtually docked compounds were built and energy minimized. The best obtained studied poses were chosen for docking using CDOCKER energy and were inspected in 3D and 2D styles.

Firstly, redocking of the ligand, benzimidazol-2-ylurea, was carried out to validate the docking protocol. The RMSD value was 0.825 (less than 2) which indicates the validity and confidence in the obtained docking results. As shown in Fig. 4**A and 4B**, benzimidazol-2-ylurea (CDOCKER energy = −45.0109 and CDOCKER interaction energy = −58.2929), incorporated in the formation of 2 hydrogen bonds with Asp73 and Arg136. Also, benzimidazol-2-ylurea formed many hydrophobic interactions such as van der Waals, Carbon Hydrogen bond and Pi-Alkyl interactions with Val43, Asn46, Val71, Asp73, Arg76, Gly77, Ile78, Pro79, Lys103, Arg136 and Val167 amino acid residues.

Novobiocin, as illustrated in Fig. 5**A and 5B**, with CDOCKER energy = −11.1743 and CDOCKER interaction energy = −69.805, engaged in 3 hydrogen bonds with Asp73, Arg136 and Thr165. In addition to other hydrophobic interactions such as van der Waals, Salt Bridge, Attractive Charge, Carbon Hydrogen bond, Pi-Cation, Alkyl and Pi-Alkyl interactions with Arg76, Ile78, Pro79, Ile94, Lys103, Arg136 and Val120 amino acid residues.

Ciprofloxacin, as illustrated in Fig. 5**C and 5D**, with CDOCKER energy = −26.2818 and CDOCKER interaction energy = −54.2711, engaged in 4 hydrogen bonds with Gly77, Arg136 (two hydrogen bonds) and many other hydrophobic interactions such as van der Waals, Attractive Charge, Carbon Hydrogen bond, Halogen (Fluorine), Pi-Cation, Pi-anion, Alkyl and Pi-Alkyl interactions with Asn46, Glu50, Arg76, Ile78, Pro79, Ile94, Lys103 and Arg136 amino acid residues.

The docking results of compound **6c** (CDOCKER energy = −24.1222 and CDOCKER interaction energy = −50.4697), (Fig. 6**A and 6B**), revealed that it formed 3 hydrogen bonds; the nitrogen atom of 1,2,4-oxadizaole nucleous forms one hydrogen bond with Arg136, and the oxygen atom 1,3-peopenone moiety engaged in two hydrogen bonds with Arg67 and Gly77. Also **6c** showed many hydrophobic interactions such as van der Waals, Carbon Hydrogen bond, Pi-Cation, Pi-Sigma and Pi-Alkyl interactions with Ala47, Ile78, Pro79, Ile82, Ala90 and Lys103 amino acid residues.

The docking result of compound **7c**, (Fig. 6**C and 6D**) (CDOCKER

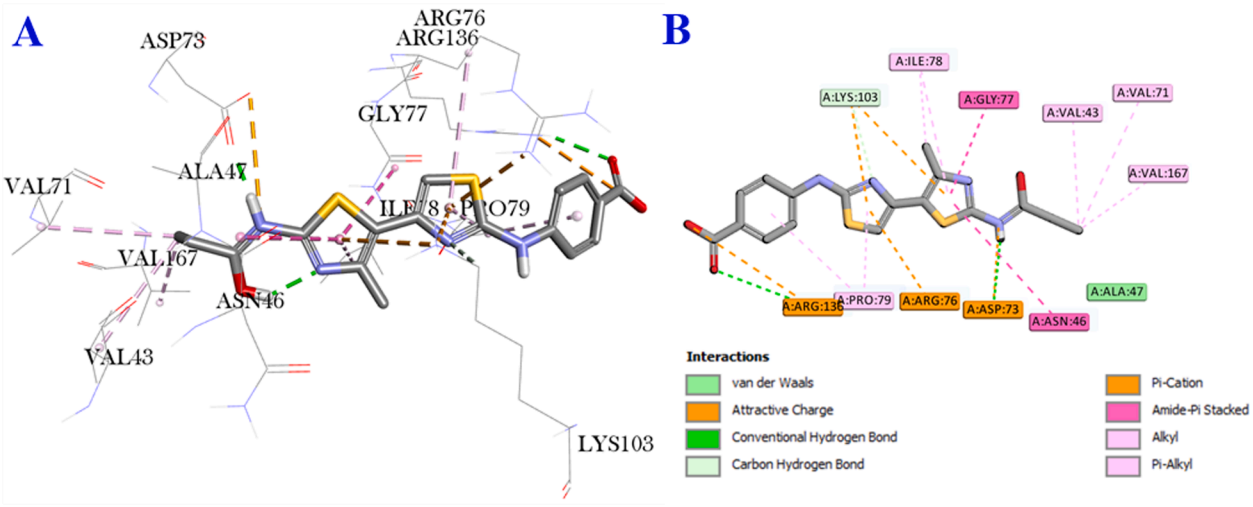

Fig. 4. Binding mode of benzimidazol-2-ylurea inhibitor into DNA gyrase pocket (PDB code: 4DUH). (**A**) 3D structure of benzimidazol-2-ylurea (grey), (**B**) 2D structure of benzimidazol-2-ylurea (grey).

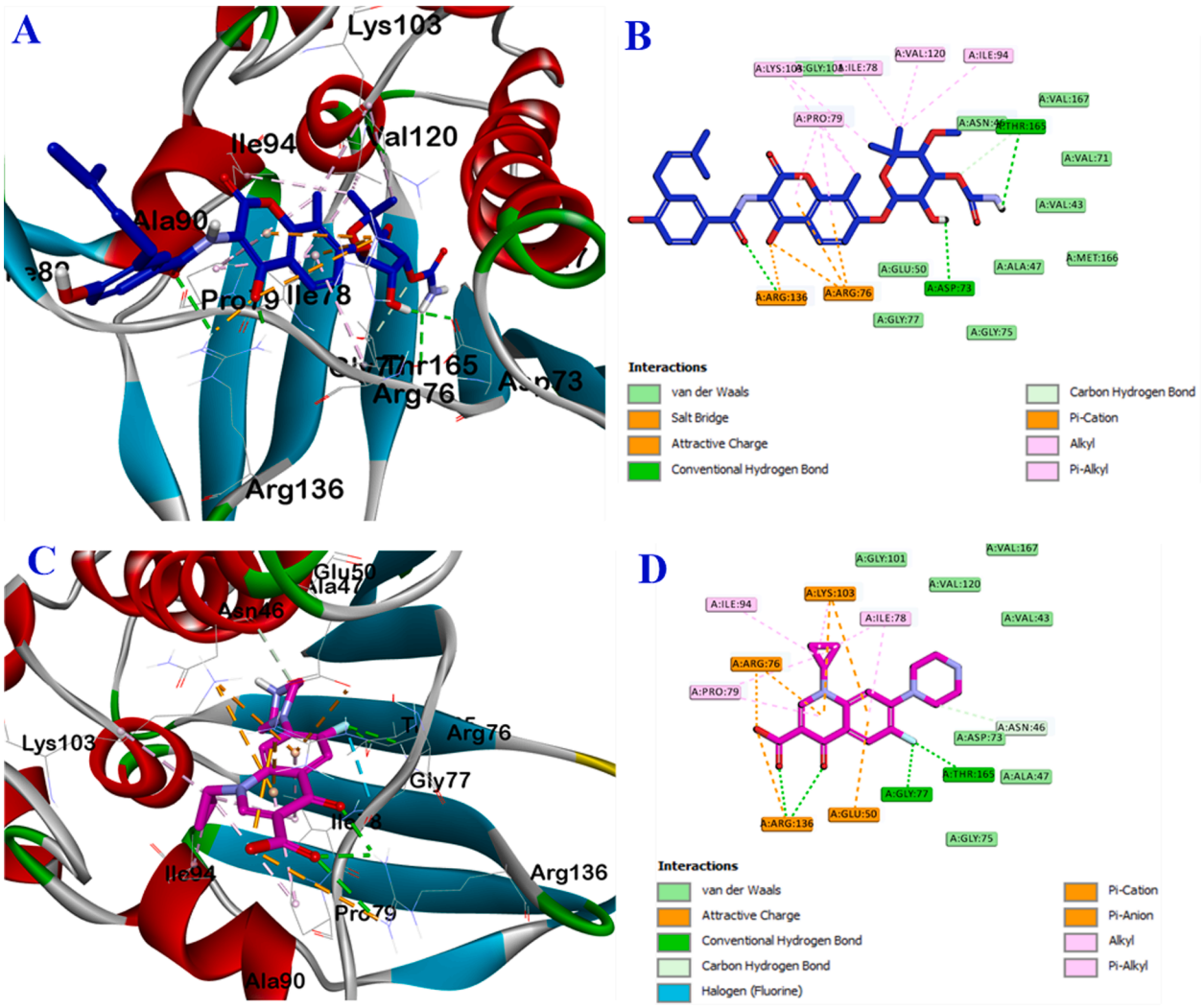

Fig. 5. Binding mode of novobiocin and ciprofolxacin into DNA gyrase pocket (PDB code: 4DUH). (**A**) 3D structure of novobiocin (blue), (**B**) 2D structure of novobiocin (blue), (**C**) 3D structure of ciprofloxacin (pink), (**D**) 2D structure of ciprofloxacin (pink). (For interpretation of the references to colour in this figure legend, the reader is referred to the web version of this article.)

energy = −16.0866 and CDOCKER interaction energy = −46.169), showed that it formed 3 hydrogen bonds; the oxygen atom of the methylene group incorporated in one hydrogen bond with Lys103, the proton of the oxime group formed one hydrogen bond with Arg136 and the oxygen atom of the oxime group engaged in the third hydrogen bond with Arg136. Further, **7c** showed many hydrophobic interactions such as van der Waals, Carbon Hydrogen bond, Pi-Cation and Pi-Alkyl interactions with Arg76, Ile78, Pro79, Ile94, Lys103 and Val120 amino acid residues.

From the docking results, it clear that hybrids **6c** and **7c** exhibited binding patterns similar to that described for the majority of gyrase B inhibitors. Thus, it could be concluded that compounds **6c** and **7c** are entitled to be used as future lead template for identifying more potent antibacterial candidates.

2.5. In silico prediction of physicochemical properties and pharmacokinetic profile

2.5.1. Lipinski rule calculations and ADMET analysis

Prediction of the physicochemical characters, pharmacokinetics and toxicity is an important tool in drug discovery of biologically active agents [32,43]. Many potential therapeutic candidates fail to reach the clinic due to their unfavorable absorption, distribution, metabolism, elimination and toxic (ADMET) factors [44]. Thus, utilizing the online application Pre-ADMET, theoretical calculations of the pharmacokinetic parameters as well as the theoretical agreement of compounds **6c**, **7c**, ciprofloxacin and novobiocin to both Lipinski's Rule of Five [45] and Veber's standard [46] were carried out.

The obtained results as illustrated in Table 3, showed that compounds **6c** and **7c** are in agreement with Lipinski's rule with only one violation Log P > 5). Moreover, all the tested compounds had TPSA values <140 $Å^2$ which used to calculate the percentage of oral absorption (%ABS) using the following equation: (%ABS = 109-(0.345 TPSA) [47]. The tested compounds **6c** and **7c** exhibited better oral absorption than than both ciprofloxacin and novobiocin with %ABS of 85.93, 80.32, 79.40 and 55.73, respectively.

Absorption is the process by which the drug can reach the systemic circulation through body organs via several routes such as oral absorption (human intestinal absorption, HIA), skin permeability (SP, LogKp) and permeability through certain cells such as MDCK and Caco2 cells [48].

Moreover, compounds **6c** (98.22%) and **7c** (96.89%) displayed good intestinal absorption with HIA values close to 1 (acceptable range: 0–100% absorption) which is similar to ciprofloxacin (96.27%) and better than novobiocin (71.71%). Skin permeability (SP, LogKp) was found to be slightly less than the acceptable range (−2.5 LogKp)

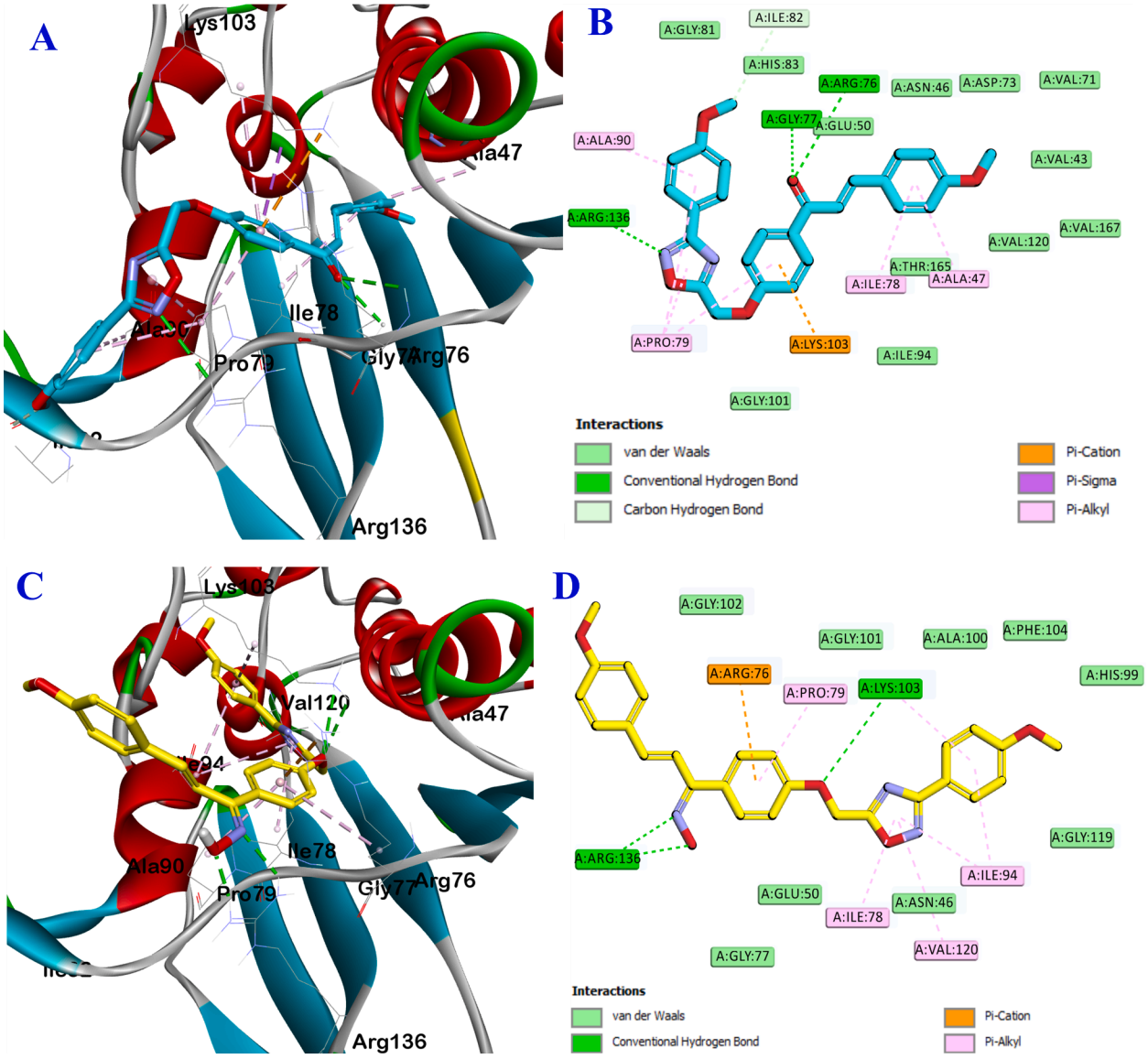

Fig. 6. Binding mode of compounds **6c** and **7c** into DNA gyrase pocket (PDB code: 4DUH). (**A**) 3D structure of **6c** (cyan), (**B**) 2D structure of **6c** (cyan), (**C**) 3D structure of **7c** (yellow), (**D**) 2D structure of **7c** (yellow). (For interpretation of the references to colour in this figure legend, the reader is referred to the web version of this article.)

Table 3
Calculated parameters of Veber's and Lipinski's rule of five for compounds **6c**, **7c** ciprofloxacin and novobiocin.

Comp.	MW	Log P	HBD	HBA	nVs	MolPSA	%ABS	Drug likeness score
Lipinski*	≤500	≤5	≤5	≤10	≤1	–	–	
Veber**	–	–	–	–	–	≤140	–	
6c	442.15	5.46	0	7	1	66.87 A^2	85.93	−0.31
7c	457.16	6.01	1	8	1	83.13 A^2	80.32	0.06
Ciprofloxacin	331.13	0.45	2	4	0	58.80 A^2	79.40	0.84
Novobiocin	612.23	3.10	6	11	1	154.40 A^2	55.73	1.11

* Reference values of Lipinski;
** Reference values of Veber; MW, Molecular weight; LogP, lipophilicity (O/W); HBD, Number of hydrogen bond donors; HBA, Number of hydrogen bond acceptors; nVs, Number of Lipinski rule violations; MolPSA, molecular polar surface area (PSA) (Å2); %ABS, percentage of oral absorption.

(Table 4).

Regarding distribution (Table 4), two parameters namely; blood brain barrier (BBB) and plasma binding protein (PBP), were measured to predict the distribution of molecules from one organ to another. BBB allows the hydrophobic and small molecules to diffuse to the brain which considered as an important predictor for the discovery of central nervous system (CNS) drugs. Additionally, measurement of the percentage of a molecule bound to plasma protein (PPB%) is also helpful in estimation of the novel target compounds distribution. Results exhibited that compounds **6c** (99.19) and **7c** (97.29) showed strong plasm protein binding values indicating prolonged half-lives more than ciprofloxacin (31.05) and novobiocin (84.66). Moreover, compounds **6c** (0.157) and

Table 4
Pharmacokinetic properties and toxicity prediction of compounds **6c**, **7c** ciprofloxacin and novobiocin.

	Absorption			Distribution				Metabolism				Toxicity			
Compound	HIA (%)	Caco2	SP_LogKp	MDCK	PPB %	BBB	2C19	2C9	2D6	3A4	Pgp_inhibition	AMES	Carcino_Mouse	Carcino_Rat	hERG_inhibition
6c	98.22	51.85	−2.40	26.18	99.19	0.157	Yes	Yes	No	Yes	No	Mutagen	Negative	Negative	Medium
7c	96.89	28.59	−2.25	22.99	97.29	0.019	Yes	Yes	No	Yes	inhibitor	Mutagen	Negative	Negative	Medium
Ciprofloxacin	96.27	21.28	−4.59	10.30	31.05	0.014	No	No	No	No	No	Mutagen	Negative	Negative	Low
Novobiocin	71.71	13.08	−3.45	0.04	84.66	0.065	No	Yes	No	Yes	No	Mutagen	Positive	Negative	High

7c (0.019) showed limited brain penetration (BBB; unbound brain -to-plasma ratio) as well as both ciprofloxacin (0.014) and novobiocin (0.065).

Concerning metabolism (Table 4), the chemical modification(S) or the biotransformation of xenobiotics or exogenous compounds to facilitate their excretion through increasing their water solublity either in phase I or phase II. Cytochrome P450 isoforms predicts the ability of compounds to be inhibitors for drug metabolizing enzymes such as CYP2C19, CYP2C9, CYP2D6, CYP3A4, CYP1A2. Furthermore, glycoprotein (P-gp) inhibition measurement is used to predict the excretion property of the target compounds. In this study, compounds **6c** and **7c** exhibited good inhibitory behavior towards CYP2C19, CYP2C9 and CYP3A4, but they did not show inhibitory behavior towards CYP2D6. Moreover, compound **6c** had no inhibitory effect on P-gp, while **7c** is P-gp inhibitor.

Finally, toxicity prediction (Table 4) of compounds **6c**, **7c**, ciprofloxacin and novobiocin was obtained by measuring AMES test (for mutagenicity prediction), carcino-Mouse/Rat (for carcinogenicity prediction of the tested compounds) and hERG-inhibition (for checking the cardiac toxicity). Compounds **6c** and **7c**, ciprofloxacin and novobiocin showed mutagenic behavior in AMES test. All compounds had negative carcinogenic effect in mouse and rats except novobiocin which had positive carcinogenic effect in mouse. Compounds **6c** and **7c** showed medium risk as cardiotoxic agents better than novobiocin which exhibited high risk as cardiotoxic agents. From these predicted ADMET parameters, we could conclude that compounds **6c** and **7c** have acceptable physicochemical properties and reasonable drug-likeness, hence, can be used as a promising drug candidate for development of new antibacterial agents.

3. Conclusion

In summary, a novel series of 1,2,4-oxadiazole appended chalcone **6a-f** and their oxime counterpart**s 7a-f** were prepared and evaluated for their *in vitro* quantitative (MIC) antimicrobial activity by the modified agar diffusion method in Müller-Hinton Broth and Sabouraud Liquid Medium. Among all, compounds, **6a**, **6c-e**, **7b** and **7e** proved to possess broad spectrum antibacterial activity against the tested Gram-positive and Gram-negative organisms. Compound **6a** (against *S. aureus*), **6c** (against *B. subtilis* and *E. hirae*), **6e** (against *E. hirae*), **6f**, **7a** and **7c** (against *E. coli*),**7d** (against *B. subtilis*) all with MIC value of 3.12 μM were two-fold more active than the standard ciprofloxacin (MIC = 6.25 μM). In comparison with novobiocin (IC_{50} = 12.3 μM) and ciprofloxacin (IC_{50} = 10.5 μM), *E-coli* gyrase inhibitory activity assessment of the synthesized target compounds showed that compounds **6c**, **7c**, **7e** and **7b** displayed a good inhibitory activity against *E-coli* gyrase with IC_{50} values of 17.05 μM, 13.4 μM, 16.9 μM, and 19.6 μM, respectively. The docking study exhibited that both compounds **6c** and **7c** showed binding patterns similar to that described for the majority of gyrase B inhibitors. Furthermore, hybrids **6c** and **7c** exhibited acceptable physicochemical properties and good drug-likeness scores. Therefore, compound **6c** and **7c** could be considered as promising leads as antibacterial candidate which merit further optimization and development in future work for potent derivatives.

4. Experimental

4.1. Chemistry

4.1.1. General information

All commercially available reagents were purchased from Merck, Aldrich and Fluka and were used without further purification. All reactions were monitored by thin layer chromatography (TLC) using precoated plates of silica gel G/UV-254 of 0.25 mm thickness (Merck 60F254) using UV light (254 nm/365 nm) for visualization. Melting points were detected with a Kofler melting points apparatus and

uncorrected. Infrared spectra were recorded with a FT-IR-ALPHBROKER-Platinum-ATR spectrometer and are given as cm^{-1} using the attenuated total reflection (ATR) method. ^1H NMR and ^{13}C NMR spectra for all new compounds were recorded in $CDCl_3$ or DMSO-d_6 on a Bruker Bio Spin AG spectrometer at 400 MHz and 100 MHz, respectively. For ^1H NMR, chemical shifts (δ) were given in parts per million (ppm) with reference to tetramethylsilane (TMS) as an internal standard ($\delta = 0$); coupling constants (J) were given in hertz (Hz) and data are reported as follows: chemical shift, integration, multiplicity (s = singlet, d = doublet, m = multiplet). For ^{13}C NMR, TMS ($\delta = 0$), DMSO (δ = 39.51) or $CDCl_3$ (δ = 77.2) was used as internal standard and spectra were obtained with complete proton decoupling. Elemental analyses were obtained on a Perkin-Elmer CHN-analyzer model. Compounds **3** [22], **4a-f** and **5a-f** [32,33,35] were prepared according to the previously reported procedure.

4.1.2. General procedure for the synthesis of (2E)-3-(4-methoxyphenyl)-1-{4-[(3-aryl-1,2,4-oxadiazol-5-yl)methoxy]phenyl}prop-2-en-1-one ***(6a-f)***

To a suspension of {4-[(2*E*)-3-(4-methoxyphenyl)prop-2-enoyl]phenoxy}acetic acid (**3**, 2 mmol, 0.624 g) in acetonitrile (30 mL), the *N,N′*-carbonyldiimidazole (CDI) (2.2 mmol, 0.36 g) was added and the mixture was stirred at room temperature for 30 mins. The appropriate amidoximes **4a-f** (2 mmol) was then added and stirring was continued for additional 2 h. The reaction mixture was heated under reflux overnight (monitored with TLC). The reaction mixture was allowed to cool to room temperature and the obtained precipitate was filtered, dried and recrystallized from methanol to afford **6a-f.**

4.1.2.1. (2E)-3-(4-Methoxyphenyl)-1-{4-[(3-phenyl-1,2,4-oxadiazol-5-yl)methoxy]phenyl}prop-2-en-1-one (6a). Yield 78%; white crystal; m.p.: 143–145 °C. IR (ATR) ν_{max} 3051 (C—H aromatic), 2957, 2934, 2906, 2836 (C—H aliphatic), 1661 (C═O), 1603 (C═N) cm^{-1}. ^1H NMR (400 MHz, $CDCl_3$) δ 3.87 (s, 3H, OCH_3), 5.45 (s, 2H, CH_2), 6.95 (d, J = 7.4 Hz, 2H, $CH_{arom.}$), 7.14 (d, J = 7.6 Hz, 2H, $CH_{arom.}$), 7.42 (d, J = 15.5 Hz, 1H, $CH_{arom.}$), 7.51–7.53 (m, 3H, $CH_{arom.}$), 7.61 (d, J = 7.4 Hz, 2H, $CH_{arom.}$), 7.80 (d, J = 15.5 Hz, 1H, $CH_{arom.}$), 8.06–8.13 (m, 4H, $CH_{arom.}$); ^{13}C NMR (100 MHz, $CDCl_3$) δ 55.4, 61.0, 114.5, 114.7, 119.6, 126.3, 127.6, 127.8, 128.9, 130.1, 130.8, 131.5, 133.0, 144.3, 160.9, 161.7, 168.7, 174.2, 188.7. Anal. Calcd. for $C_{25}H_{20}N_2O_4$ (412.43): C, 72.80; H, 4.89; N, 6.79. Found: C, 72.67; H, 4.77; N, 6.86.

4.1.2.2. (2E)-3-(4-Methoxyphenyl)-1-{4-[(3-(4-chlorophenyl)-1,2,4-oxadiazol-5-yl)methoxy] phenyl}prop-2-en-1-one (6b). Yield 83%; white crystal; m.p.: 162–164 °C. IR (ATR) ν_{max} 3073, 3051 (C—H aromatic), 2997, 2961, 2933, 2834 (C—H aliphatic), 1652 (C═O), 1599 (C═N) cm^{-1}. ^1H NMR (400 MHz, DMSO-d_6) δ 3.83 (s, 3H, OCH_3), 5.76 (s, 2H, CH_2), 7.02 (d, J = 8.6 Hz, 2H, $CH_{arom.}$), 7.26 (d, J = 8.7 Hz, 2H, $CH_{arom.}$), 7.66 (d, J = 8.6 Hz, 2H, $CH_{arom.}$), 7.71–7.85 (m, 4H, $CH_{arom.}$), 8.04 (d, J = 8.5 Hz, 2H, $CH_{arom.}$), 8.18 (d, J = 8.7 Hz, 2H, $CH_{arom.}$); ^{13}C NMR (100 MHz, DMSO-d_6) δ 55.9, 61.5, 114.9, 115.3, 120.0, 125.1, 127.9, 129.4, 130.0, 131.2, 131.3, 132.4, 137.1, 143.9, 161.4, 161.8, 167.5, 176.2, 187.9. Anal. Calcd. for $C_{25}H_{19}ClN_2O_4$ (446.88): C, 67.19; H, 4.29; N, 6.27. Found: C, 67.57; H, 4.01; N, 6.13.

4.1.2.3. (2E)-3-(4-Methoxyphenyl)-1-{4-[(3-(4-methoxyphenyl)-1,2,4-oxadiazol-5-yl)methoxy] phenyl}prop-2-en-1-one (6c). Yield 81%; beige solid; m.p.: 169–171 °C. IR (ATR) ν_{max} 3069, 3019 (C—H aromatic), 2997, 2941, 2836 (C—H aliphatic), 1652 (C═O), 1600 (C═N) cm^{-1}. ^1H NMR (400 MHz, DMSO-d_6) δ 3.83 (s, 6H, $2OCH_3$), 5.72 (s, 2H, CH_2), 7.02–7.26 (m, 6H, $CH_{arom.}$), 7.71–8.20 (m, 8H, $CH_{arom.}$); ^{13}C NMR (100 MHz, DMSO-d_6) δ 55.8, 55.9, 61.5, 114.9, 115.3, 118.5, 120.0, 127.9, 129.3, 131.2, 131.3, 132.4, 143.9, 161.4, 161.8, 162.4, 166.1, 168.0, 175.5, 187.9. Anal. Calcd. for $C_{26}H_{22}N_2O_5$ (442.46): C, 70.58; H, 5.01; N, 6.33. Found: C, 70.72; H, 4.92; N, 6.24.

4.1.2.4. (2E)-3-(4-Methoxyphenyl)-1-{4-[(3-(3,4-dimethoxyphenyl)-1,2,4-oxadiazol-5-yl)metho-xy]phenyl}prop-2-en-1-one (6d). Yield 82%; beige solid; m.p.: 146–148 °C. IR (ATR) ν_{max} 3067, 3032 (C—H aromatic), 2990, 2964, 2913, 2839 (C—H aliphatic), 1651 (C═O), 1601 (C═N) cm^{-1}. ^1H NMR (400 MHz, $CDCl_3$) δ3.87 (s, 3H, OCH_3), 3.97 (s, 3H, OCH_3), 3.98 (s, 3H, OCH_3), 5.43 (s, 2H, CH_2), 6.95–6.99 (m, 3H, $CH_{arom.}$), 7.14 (d, J = 7.1 Hz, 2H, $CH_{arom.}$), 7.41 (d, J = 15.6 Hz, 1H, $CH_{arom.}$), 7.61 (br. s, 3H, $CH_{arom.}$), 7.74 (d, J = 7.1 Hz, 1H, $CH_{arom.}$), 7.80 (d, J = 15.6 Hz, 1H, $CH_{arom.}$), 8.07 (d, J = 6.8 Hz, 2H, $CH_{arom.}$); ^{13}C NMR (100 MHz, $CDCl_3$) δ 55.4, 56.0, 56.1, 61.1, 110.2, 111.3, 114.5, 114.7, 118.8, 119.5, 121.2, 127.8, 130.1, 130.8, 132.9, 144.3, 149.4, 151.9, 160.9, 161.7, 168.5, 173.9, 188.7. Anal. Calcd. for $C_{27}H_{24}N_2O_6$ (472.48): C, 68.63; H, 5.12; N, 5.93. Found: C, 68.47; H, 5.03; N, 5.77.

4.1.2.5. (2E)-3-(4-Methoxyphenyl)-1-{4-[(3-(4-nitrophenyl)-1,2,4-oxadiazol-5-yl)methoxy] phenyl}prop-2-en-1-one (6e). Yield 79%; yellow solid; m.p.: 190–192 °C. IR (ATR) ν_{max} 3072, 3050 (C—H aromatic), 2978, 2939, 2840 (C—H aliphatic), 1650 (C═O), 1599 (C═N) cm^{-1}. ^1H NMR (400 MHz, DMSO-d_6) δ 3.82 (s, 3H, OCH_3), 5.79 (s, 2H, CH_2), 7.01 (d, J = 8.6 Hz, 2H, $CH_{arom.}$), 7.27 (d, J = 7.4 Hz, 2H, $CH_{arom.}$), 7.67–7.85 (m, 4H, $CH_{arom.}$), 8.18–8.42 (m, 6H, $CH_{arom.}$); ^{13}C NMR (100 MHz, DMSO-d_6) δ 55.9, 61.5, 114.9, 115.3, 120.0, 125.0, 127.9, 129.1, 131.2, 131.3, 132.0, 132.4, 143.9, 149.9, 161.3, 161.8, 167.1, 176.7, 187.9. Anal. Calcd. for $C_{25}H_{19}N_3O_6$ (457.43): C, 65.64; H, 4.19; N, 9.19. Found: C, 65.78; H, 4.00; N, 9.34.

4.1.2.6. (2E)-3-(4-Methoxyphenyl)-1-{4-[(3-(2-naphthyl)-1,2,4-oxadiazol-5-yl)methoxy] phenyl}prop-2-en-1-one (6f). Yield 80%; beige solid; m.p.: 172–174 °C. IR (ATR) ν_{max} 3079, 3049 (C—H aromatic), 2962, 2912, 2839 (C—H aliphatic), 1659 (C═O), 1594 (C═N) cm^{-1}. ^1H NMR (400 MHz, DMSO-d_6) δ 3.83 (s, 3H, OCH_3), 5.79 (s, 2H, CH_2), 7.02 (d, J = 8.1 Hz, 2H, $CH_{arom.}$), 7.29 (d, J = 8.3 Hz, 2H, $CH_{arom.}$), 7.61–7.78 (m, 4H, $CH_{arom.}$), 7.84 (d, J = 8.5 Hz, 2H, $CH_{arom.}$), 8.01–8.16 (m, 4H, $CH_{arom.}$), 8.20 (d, J = 8.3 Hz, 2H, $CH_{arom.}$), 8.67 (s, 1H, $CH_{arom.}$); ^{13}C NMR (100 MHz, DMSO-d_6) δ 55.9, 61.6, 114.9, 115.3, 120.1, 123.6, 123.8, 127.6, 127.9, 128.2, 128.3, 128.5, 129.4, 129.6, 131.1, 131.3, 132.4, 133.1, 134.8, 143.9, 161.4, 161.8, 168.4, 176.0, 187.9. Anal. Calcd. for $C_{29}H_{22}N_2O_4$ (462.49): C, 75.31; H, 4.79; N, 6.06. Found: C, 75.72; H, 4.55; N, 6.22.

4.1.3. General procedure for the synthesis of (2E)-3-(4-methoxyphenyl)-1-{4-[(3-aryl-1,2,4-oxadiazol-5-yl)methoxy]phenyl}prop-2-en-1-one oxime (7a-f)

A mixture of 1,2,4-oxadiazole derivatives **6a-f** (0.7 mmole) and hydroxylamine hydrochloride (2.1 mmole, 0.15 g) in 20 mL pyridine was stirred at 70 °C for 3 hrs. After cooling, the mixture was added onto ice cold distilled water and acidified by conc. HCl. The formed crude product **7a-f** was then collected by filtration, washed with distilled water, dried and recrystallized from methanol.

4.1.3.1. 3-(4-Methoxyphenyl)-1-{4-[(3-phenyl-1,2,4-oxadiazol-5-yl) methoxy]phenyl}prop-2-en-1-one oxime (7a). Yield 72%; white solid; m.p.: 140–142 °C. Spectral data for the major isomer: IR (ATR) ν_{max} 3310 broad (O—H), 3058, 3004 (C—H aromatic), 2958, 2931, 2836 (C—H aliphatic), 1604 (C═N) cm^{-1}. ^1H NMR (400 MHz, DMSO-d_6) δ 3.78 (s, 3H, OCH_3), 5.66 (s, 2H, CH_2), 6.69 (d, J = 16.6 Hz, 1H, $CH_{arom.}$), 6.88–6.97 (m, 2H, $CH_{arom.}$), 7.27 (d, J = 8.5 Hz, 1H, $CH_{arom.}$), 7.39–7.51 (m, 3H, $CH_{arom.}$), 7.59–7.65 (m, 5H, $CH_{arom.}$), 8.02–8.05 (m, 3H, $CH_{arom.}$), 11.36 (s, 1H, OH); ^{13}C NMR (100 MHz, DMSO-d_6) δ 55.7, 61.4, 114.7 (2C), 114.8 (2C), 115.0, 115.2, 126.3, 127.6 (2C), 128.5, 129.2 (2C), 129.8 (2C), 130.6 (2C), 132.2, 136.9, 152.7, 158.1, 159.9, 168.3, 176.2. Anal. Calcd. for $C_{25}H_{21}N_3O_4$ (427.45): C, 70.25; H, 4.95; N, 9.83. Found: C, 70.46; H, 4.74; N, 9.52.

4.1.3.2. 3-(4-Methoxyphenyl)-1-{4-[(3-(4-chlorophenyl)-1,2,4-oxadiazol-5-yl)methoxy] phenyl}prop-2-en-1-one oxime (7b). Yield 77%; white solid; m.p.: 190–192 °C. Spectral data for the major isomer: IR (ATR) ν_{max} 3263 broad (O—H), 3060, 3007 (C—H aromatic), 2962, 2933, 2836 (C—H aliphatic), 1605 (C=N) cm^{-1}. ^{1}H NMR (400 MHz, DMSO-d_6) δ 3.78 (s, 3H, OCH_3), 5.66 (s, 2H, CH_2), 6.68 (d, J = 17.6 Hz, 1H, $CH_{arom.}$), 6.93–6.95 (d, J = 8.4 Hz, 2H, $CH_{arom.}$), 7.17 (d, J = 8.4 Hz, 2H, $CH_{arom.}$), 7.42–7.50 (m, 5H, $CH_{arom.}$), 7.66 (d, J = 8.3 Hz, 2H, $CH_{arom.}$), 8.05 (d, J = 8.3 Hz, 2H, $CH_{arom.}$), 11.36 (s, 1H, OH); ^{13}C NMR (100 MHz, DMSO-d_6) δ 55.7, 61.4, 114.8 (2C), 115.2 (2C), 116.0, 125.2, 129.1, 129.4 (2C), 129.8 (2C), 130.0 (2C), 130.6 (2C), 136.9, 137.0, 155.4, 158.1, 160.5, 167.5, 176.5. Anal. Calcd. for $C_{25}H_{20}ClN_3O_4$ (461.89): C, 65.01; H, 4.36; N, 9.10. Found: C, 64.87; H, 4.27; N, 9.03.

4.1.3.3. 3-(4-Methoxyphenyl)-1-{4-[(3-(4-methoxyphenyl)-1,2,4-oxadiazol-5-yl)methoxy] phenyl}prop-2-en-1-one oxime (7c). Yield 74%; beige solid; m.p.: 154–155 °C. Spectral data for the major isomer: IR (ATR) ν_{max} 3281 broad (O—H), 3061, 3003 (C—H aromatic), 2962, 2937, 2836 (C—H aliphatic), 1604 (C=N) cm^{-1}. ^{1}H NMR (400 MHz, DMSO-d_6) δ 3.82 (s, 3H, OCH_3), 3.83 (s, 3H, OCH_3), 5.61 (s, 2H, CH_2), 6.63–7.49 (m, 10*H*, $CH_{arom.}$), 7.62 (d, J = 8.8 Hz, 1H, $CH_{arom.}$), 7.94–7.97 (m, 3H, $CH_{arom.}$), 11.46 (s, 1H, OH); ^{13}C NMR (100 MHz, DMSO-d_6) δ 55.7, 55.9, 61.3, 114.8 (2C), 115.1 (2C), 115.2 (2C), 115.8, 118.4, 127.5, 129.2 (2C), 129.3 (2C), 130.7 (2C), 137.0, 152.9, 155.5, 158.1, 160.4, 162.3, 167.9, 175.8. Anal. Calcd. for $C_{26}H_{23}N_3O_5$ (457.47): C, 68.26; H, 5.07; N, 9.19. Found: C, 68.58; H, 4.95; N, 9.04.

4.1.3.4. 3-(4-Methoxyphenyl)-1-{4-[(3-(3,4-dimethoxyphenyl)-1,2,4-oxadiazol-5-yl)methoxy]phenyl}prop-2-en-1-one oxime (7d). Yield 70%; beige solid; m.p.: 155–157 °C. Spectral data for the major isomer: IR (ATR) ν_{max} 3277 broad (O—H), 3059, 3005 (C—H aromatic), 2964, 2936, 2838 (C—H aliphatic), 1605 (C=N) cm^{-1}. ^{1}H NMR (400 MHz, DMSO-d_6) δ 3.85 (s, 9H, $3OCH_3$), 5.63 (s, 2H, CH_2), 6.68 (d, J = 16.4 Hz, 1H, $CH_{arom.}$), 6.94 (d, J = 7.6 Hz, 2H, $CH_{arom.}$), 7.09–7.16 (m, 4H, $CH_{arom.}$), 7.42–7.51 (m, 6H, $CH_{arom.}$), 11.36 (s, 1H, OH); ^{13}C NMR (100 MHz, DMSO-d_6) δ 55.7, 56.2 (2 OCH_3), 61.5, 110.4, 112.6, 114.8 (2C), 115.2 (2C), 116.0, 118.6, 121.1, 127.7, 129.1, 129.8 (2C), 130.6 (2C), 136.9, 149.6, 152.2, 155.4, 158.2, 160.5, 168.1, 175.8. Anal. Calcd. for $C_{27}H_{25}N_3O_6$ (487.50): C, 66.52; H, 5.17; N, 8.62. Found: C, 66.67; H, 5.00; N, 8.69.

4.1.3.5. 3-(4-Methoxyphenyl)-1-{4-[(3-(4-nitrophenyl)-1,2,4-oxadiazol-5-yl)methoxy] phenyl}prop-2-en-1-one oxime (7e). Yield 72%; yellow solid; m.p.: 162–164 °C. Spectral data for the major isomer: IR (ATR) ν_{max} 3347 broad (O—H), 3072, 3036 (C—H aromatic), 2958, 2934, 2838 (C—H aliphatic), 1604 (C=N) cm^{-1}. ^{1}H NMR (400 MHz, DMSO-d_6) δ 3.78 (s, 3H, OCH_3), 5.70 (s, 2H, CH_2), 6.68 (d, J = 16.8 Hz, 1H, $CH_{arom.}$), 6.88–7.50 (m, 9H, $CH_{arom.}$), 8.31–8.45 (m, 4H, $CH_{arom.}$), 11.36 (s, 1H, OH); ^{13}C NMR (100 MHz, DMSO-d_6) δ 55.7, 61.5, 114.7 (2C), 114.8 (2C), 115.0, 115.2, 116.0, 125.0, 125.3 (2C), 128.5 (2C), 129.0, 129.1 (2C), 130.7 (2C), 132.1, 133.9, 136.9, 149.8, 167.1, 177.0. Anal. Calcd. for $C_{25}H_{20}N_4O_6$ (472.45): C, 63.56; H, 4.27; N, 11.86. Found: C, 63.74; H, 4.19; N, 11.81.

4.1.3.6. 3-(4-Methoxyphenyl)-1-{4-[(3-(2-naphthyl)-1,2,4-oxadiazol-5-yl)methoxy] phenyl}prop-2-en-1-one oxime (7f). Yield 75%; beige solid; m.p.: 180–182 °C. Spectral data for the major isomer: IR (ATR) ν_{max} 3299 broad (O—H), 3056, 3026 (C—H aromatic), 2999, 2957, 2836 (C—H aliphatic), 1604 (C=N) cm^{-1}. ^{1}H NMR (400 MHz, DMSO-d_6) δ 3.77 (s, 3H, OCH_3), 5.70 (s, 2H, CH_2), 6.69 (d, J = 16.8 Hz, 1H, $CH_{arom.}$), 6.92 (d, J = 8.7 Hz, 2H, $CH_{arom.}$), 7.19–7.68 (m, 9H, $CH_{arom.}$), 8.02 (d, J = 7.6 Hz, 1H, $CH_{arom.}$), 8.08–8.16 (m, 3H, $CH_{arom.}$), 8.68 (s, 1H, $CH_{arom.}$), 11.37 (s, 1H, OH); ^{13}C NMR (100 MHz, DMSO-d_6) δ 55.7, 61.5, 114.8 (2C), 115.2 (2C), 116.0, 123.7, 123.8, 127.6, 128.2, 128.3, 128.4, 128.5, 129.1, 129.4, 129.6, 129.8, 130.7 (2C), 133.1 (2C), 134.8, 136.9, 155.4, 158.2, 160.4, 168.4, 176.3. Anal. Calcd. for $C_{29}H_{23}N_3O_4$ (477.51): C, 72.94; H, 4.85; N, 8.80. Found: C, 73.47; H, 4.93; N, 8.72.

4.2. Biological assays

4.2.1. Antimicrobial activity

All the synthesized compounds **6a-f** and **7a-f** were estimated *in vitro* for their antimicrobial activity against a board of standard strains of the Gram-negative bacteria including *Pseudomonas aeuroginosa* (ATCC-27953), *Klebsiella pneumoniae* (ATCC-13883), and *Escherichia coli* (ATCC −25922), the Gram-positive bacteria including *Bacillus subtilis* (ATCC-19659), *Staphylococcus aureus* (ATCC-25923) and *Enterococcus hirae (*ATCC-10541), and the yeast-like fungal pathogen *Candida albicans* (ATCC-10231). The antimicrobial activity of the tested compounds was carried out by means of the agar disc-diffusion method using the Müller-Hinton agar medium while a 24-hours bacterial culture was swabbed on the surface of the Muller-Hinton agar plate using a sterile cotton swab. The compounds were freshly dissolved in Dimethyl Sulfoxide (DMSO) and the twofold dilutions were prepared. The sterile filter discs (9 mm) were separately loaded with 100 ul of prepared compounds and left till dryness and then positioned on a previously inoculated nutrient agar with the target microbial strain. After two hours of diffusion at 4 °C, the plates were incubated at 37 °C for 24 h regarding bacteria and 48 h regarding Candida albicans. and the inhibition areas were measured and compared to sulphamethoxazole (SXT) as the reference antibiotic. The minimal inhibitory concentration (MIC) was estimated as the minimum concentration of antimicrobial agent that totally inhibited the colony formation *via* the modified agar diffusion method in Müller-Hinton Broth and Sabouraud Liquid Medium [49–51].

4.2.2. DNA-Gyrase supercoiling inhibition assay

All compounds were screened *in vitro* for their inhibitory activity of *E. coli* DNA Gyrase supercoiling using *E. coli* DNA gyrase microplate assay kit (Inspiralis, Norwich, UK) according to the manufacturer's protocol [52]. Two reference drugs; ciprofloxacin and novobiocin were used. The whole tested compounds at concentrations of 100, 50, 25, 13 and 6 uM were used. The results are depicted as IC_{50} values.

4.2.3. Cell viability and MTT assay

MTT assay was performed to explore the effect of the synthesized compounds on the viability of mammary epithelial cells (MCF-10A) according to previously reported procedures [42] (*see* **Supporting Information**).

4.2.4. Docking methodology

For molecular docking analysis, Discovery Studio 2.5 software (Accelrys Inc., San Diego, CA, USA) was used for docking analysis. Fully automated docking tool using "Dock ligands (CDOCKER)" protocol running on Intel (R) core (TM) i32370 CPU @ 2.4 GHz 2.4 GHz, RAM Memory 2 GB under the Windows 7.0 system. The co-crystal structure of *E. coli* DNA gyrase B with a thiazole inhibitor (PDB code: 4DUH) was retrieved from protein data bank (https://www.rcsb.org/structure/4DUH). The docked compounds were built using Chem. 3D ultra 12.0 software [Chemical Structure Drawing Standard; Cambridge Soft corporation, USA (2010)], and copied to Discovery Studio 2.5 software. Automatic protein preparation module was used applying MMFF94 force field. The binding site sphere has been defined automatically by the software. Now the above prepared receptor is given as input for "input receptor molecule" parameter in the CDOCKER protocol parameter explorer. Force fields are applied on compounds to get the minimum lowest energy structure. The obtained poses were studied and the poses showing best ligand interactions were selected and used for CDOCKER energy (protein-ligand interaction energies) calculations. Receptor–ligand interactions of the complexes were examined in 2D and 3D styles bank

4.2.5. In silico prediction of physicochemical properties and pharmacokinetic profile.

For Lipinski's rule (rule of five) and molecular property prediction, the free accesses to website (https://www.molsoft.com/servers.html) was used. Also, for Pre-ADMET estimation, the free access of website (https://preadmet.bmdrc.kr/) was utilized for estimation.

Declaration of Competing Interest

The authors declare that they have no known competing financial interests or personal relationships that could have appeared to influence the work reported in this paper.

Acknowledgments

This project was funded by the Deanship of Scientific Research (DSR), King Abdulaziz University, Jeddah, under grant N°. **(DF-452-166-1441)**. The authors, therefore, gratefully acknowledge DSR technical and financial support.

Appendix A. Supplementary material

Supplementary data to this article can be found online at https://doi.org/10.1016/j.bioorg.2021.104885.

References

[1] W. Zhang, W. Liu, X. Jiang, F. Jiang, H. Zhuang, L. Fu, Design, synthesis and antimicrobial activity of chiral 2-(substituted-hydroxyl)-3-(benzo[d]oxazol-5-yl) propanoic acid derivatives, Eur. J. Med. Chem. 46 (9) (2011) 3639–3650.
[2] F. Prestinaci, P. Pezzotti, A. Pantosti, Antimicrobial resistance: a global multifaceted phenomenon, Pathog. Glob. Health 109 (7) (2015) 309–318.
[3] G. Sanyal, P. Doig, Bacterial DNA replication enzymes as targets for antibacterial drug discovery, Expert Opin. Drug Discov. 7 (4) (2012) 327–339.
[4] P.F. Chan, V. Srikannathasan, J. Huang, H. Cui, A.P. Fosberry, M. Gu, M.M. Hann, M. Hibbs, P. Homes, K. Ingraham, J. Pizzollo, C. Shen, A.J. Shillings, C. E. Spitzfaden, R. Tanner, A.J. Theobald, R.A. Stavenger, B.D. Bax, M.N. Gwynn, Structural basis of DNA gyrase inhibition by antibacterial QPT-1, anticancer drug etoposide and moxifloxacin, Nat. Commun. 6 (2015) 10048.
[5] A. Kolarič, T. Germe, M. Hrast, C.E.M. Stevenson, D.M. Lawson, N.P. Burton, J. Vörös, A. Maxwell, N. Minovski, M. Anderluh, Potent DNA gyrase inhibitors bind asymmetrically to their target using symmetrical bifurcated halogen bonds, Nat. Commun. 12 (2021) 150.
[6] M. Durcik, T. Tomašič, N. Zidar, A. Zega, D. Kikelj, L.P. Mašič, J. Ilaš, ATP-competitive DNA gyrase and topoisomerase IV inhibitors as antibacterial agents, Expert Opin. Ther. Pat. 29 (3) (2019) 171–180.
[7] A. Kolarič, M. Anderluh, N. Minovski, Two Decades of Successful SAR-Grounded Stories of the Novel Bacterial Topoisomerase Inhibitors (NBTIs), J. Med. Chem. 63 (11) (2020) 5664–5674.
[8] C. Zhuang, W. Zhang, C. Sheng, W. Zhang, C. Xing, Z. Miao, Chalcone: A Privileged Structure in Medicinal Chemistry, Chem. Rev. 117 (2017) 7762–7810.
[9] G. Viana, M. Bandeira, F. Matos, Analgesic and antiinflammatory effects of chalcones isolated from Myracrodruon urundeuva Allemão, Phytomedicine 10 (2003) 189–195.
[10] S.H. Lee, D.H. Sohn, X.Y. Jin, S.W. Kim, S.C. Choi, G.S. Seo, 2′, 4′, 6′-Tris (methoxymethoxy) chalcone protects against trinitrobenzene sulfonic acid-induced colitis and blocks tumor necrosis factor-α-induced intestinal epithelial inflammation via heme oxygenase 1-dependent and independent pathways, Biochem. Pharmacol. 74 (6) (2007) 870–880.
[11] M. Liu, P. Wilairat, S.L. Croft, A.-C. Tan, M.-L. Go, Structure–activity relationships of antileishmanial and antimalarial chalcones, Bioorg. Med. Chem. 11 (13) (2003) 2729–2738.
[12] T. Narender, Shweta, K. Tanvir, M. Srinivasa Rao, K. Srivastava, S.K. Puri, Prenylated chalcones isolated from Crotalaria genus inhibits in vitro growth of the human malaria parasite Plasmodium falciparum, Bioorg. Med. Chem. Lett. 15 (10) (2005) 2453–2455.
[13] I.S. Arty, H. Timmerman, M. Samhoedi, H. van der Goot, Synthesis of benzylideneacetophenones and their inhibition of lipid peroxidation, Eur. J. Med. Chem. 35 (2000) 449–457.
[14] S. Mukherjee, V. Kumar, A.K. Prasad, H.G. Raj, M.E. Bracke, C.E. Olsen, S.C. Jain, V.S. Parmar, Synthetic and biological activity evaluation studies on novel 1, 3-diarylpropenones, Bioorg. Med. Chem. 9 (2) (2001) 337–345.
[15] Z. Nowakowska, A review of anti-infective and anti-inflammatory chalcones, Eur. J. Med. Chem. 42 (2) (2007) 125–137.
[16] M. Go, X. Wu, X. Liu, Chalcones: an update on cytotoxic and chemoprotective properties, Curr. Med. Chem. 12 (2005) 483–499.
[17] P.M. Sivakumar, S.K. Geetha Babu, D. Mukesh, QSAR studies on chalcones and flavonoids as anti-tuberculosis agents using genetic function approximation (GFA) method, Chem. Pharm. Bull. 55 (1) (2007) 44–49.
[18] P. Yadav, K. Lal, L. Kumar, A. Kumar, A. Kumar, A.K. Paul, R. Kumar, Synthesis, crystal structure and antimicrobial potential of some fluorinated chalcone-1,2,3-triazole conjugates, Eur. J. Med. Chem. 155 (2018) 263–274.
[19] R. Li, X. Chen, B. Gong, P.M. Selzer, Z. Li, E. Davidson, G. Kurzban, R.E. Miller, E. O. Nuzum, J.H. McKerrow, R.J. Fletterick, S.A. Gillmor, C.S. Craik, I.D. Kuntz, F. E. Cohen, G.L. Kenyon, Structure-based design of parasitic protease inhibitors, Bioorg. Med. Chem. 4 (9) (1996) 1421–1427.
[20] J.C. Trivedi, J.B. Bariwal, K.D. Upadhyay, Y.T. Naliapara, S.K. Joshi, C. C. Pannecouque, E. De Clercq, A.K. Shah, Improved and rapid synthesis of new coumarinyl chalcone derivatives and their antiviral activity, Tetrahedron Lett. 48 (48) (2007) 8472–8474.
[21] N. Tiwari, B. Dwivedi, Synthesis of some pyrazoline and isoxazolin derivatives as possible fungicides, Boll. Chim. Farm. 128 (11) (1989) 332–335.
[22] M.F.A. Mohamed, M.S.A. Shaykoon, M.H. Abdelrahman, B.E.M. Elsadek, A. S. Aboraia, G.-D. Abuo-Rahma, Design, synthesis, docking studies and biological evaluation of novel chalcone derivatives as potential histone deacetylase inhibitors, Bioorg. Chem. 72 (2017) 32–41.
[23] H.A. Abou-Zied, B.G. Youssif, M.F. Mohamed, A.M. Hayallah, M. Abdel-Aziz, EGFR inhibitors and apoptotic inducers: Design, synthesis, anticancer activity and docking studies of novel xanthine derivatives carrying chalcone moiety as hybrid molecules, Bioorg. Chem. 89 (2019), 102997.
[24] M.F.A. Mohamed, G.-D. Abuo-Rahma, Molecular targets and anticancer activity of quinoline–chalcone hybrids: literature review, RSC Adv. 10 (52) (2020) 31139–31155.
[25] K.J. Jarvill-Taylor, R.A. Anderson, D.J. Graves, A hydroxychalcone derived from cinnamon functions as a mimetic for insulin in 3T3-L1 adipocytes, J. Am. Coll. Nutr. 20 (4) (2001) 327–336.
[26] W. Dan, J. Dai, Recent developments of chalcones as potential antibacterial agents in medicinal chemistry, Eur. J. Med. Chem. 187 (2020), 111980.
[27] K. Biernacki, M. Daśko, O. Ciupak, K. Kubiński, J. Rachon, S. Demkowicz, Novel 1,2,4-Oxadiazole Derivatives in Drug Discovery, in: Pharmaceuticals (Basel, Switzerland), 2020.
[28] N.P. Rai, V.K. Narayanaswamy, T. Govender, B.K. Manuprasad, S. Shashikanth, P. N. Arunachalam, Design, synthesis, characterization, and antibacterial activity of {5-chloro-2-[(3-substitutedphenyl-1,2,4-oxadiazol-5-yl)-methoxy]-phenyl}-(phenyl)-methanones, Eur. J. Med. Chem. 45 (6) (2010) 2677–2682.
[29] N. Zidar, H. Macut, T. Tomašič, L.P. Mašič, J. Ilaš, A. Zega, P. Tammela, D. Kikelj, New N-phenyl-4, 5-dibromopyrrolamides as DNA gyrase B inhibitors, MedChemComm 10 (2019) 1007–1017.
[30] Ž. Jakopin, J. Ilaš, M. Barančoková, M. Brvar, P. Tammela, M. Sollner Dolenc, T. Tomašič, D. Kikelj, Discovery of substituted oxadiazoles as a novel scaffold for DNA gyrase inhibitors, Eur. J. Med. Chem. 130 (2017) 171–184.
[31] S.N. Dighe, T.A. Collet, Recent advances in DNA gyrase-targeted antimicrobial agents, Eur. J. Med. Chem. 199 (2020), 112326.
[32] M.F.A. Mohamed, A.A. Marzouk, A. Nafady, D.A. El-Gamal, R.M. Allam, G.E. A. Abuo-Rahma, H.I. El Subbagh, A.H. Moustafa, Design, synthesis and molecular modeling of novel aryl carboximidamides and 3-aryl-1,2,4-oxadiazoles derived from indomethacin as potent anti-inflammatory iNOS/PGE2 inhibitors, Bioorg. Chem. 105 (2020), 104439.
[33] B.G.M. Youssif, M.F.A. Mohamed, M.M. Al-Sanea, A.H. Moustafa, A. A. Abdelhamid, H.A.M. Gomaa, Novel aryl carboximidamide and 3-aryl-1,2,4-oxadiazole analogues of naproxen as dual selective COX-2/15-LOX inhibitors: Design, synthesis and docking studies, Bioorg. Chem. 85 (2019) 577–584.
[34] S.M. El-Messery, E.-S. Habib, S.T.A. Al-Rashood, G.S. Hassan, Synthesis, antimicrobial, anti-biofilm evaluation, and molecular modelling study of new chalcone linked amines derivatives, J. Enzyme Inhib. Med. Chem. 33 (1) (2018) 818–832.
[35] M.R. Albayati, M.F. Mohamed, A.H. Moustafa, Optimization of the synthesis of het/aryl-amidoximes using an efficient green chemistry, Synth. Comm. (2020) 1–15.
[36] P. Thapa, S.P. Upadhyay, W.Z. Suo, V. Singh, P. Gurung, E.S. Lee, R. Sharma, M. Sharma, Chalcone and its analogs: Therapeutic and diagnostic applications in Alzheimer's disease, Bioorg. Chem. 108 (2021), 104681.
[37] Z. Rozmer, P. Perjési, Naturally occurring chalcones and their biological activities, Phytochem. Rev. 15 (1) (2016) 87–120.
[38] A.R. Saundane, K.N. Mathada, Synthesis, characterization, and biological evaluation of some new chalcones containing indole moiety and their derivatives, Monatsh. Chem. 147 (7) (2016) 1291–1301.
[39] A. Alejo-Armijo, A.J. Parola, F. Pina, pH-Dependent Multistate System Generated by a Synthetic Furanoflavylium Compound: An Ancestor of the Anthocyanin Multistate of Chemical Species, ACS Omega 4 (2019) 4091–4100.
[40] H.I. el-Subbagh, M.A. el-Sherbeny, M.N. Nasr, F.E. Goda, F.A. Badria, Novel diarylsulphide derivatives as potential cytotoxic agents, Boll. Chim. Farm. 134 (1995) 80-84.
[41] Y.I. El-Gazzar, H.H. Georgey, S.M. El-Messery, H.A. Ewida, G.S. Hassan, M. M. Raafat, M.A. Ewida, H.I. El-Subbagh, Synthesis, biological evaluation and molecular modeling study of new (1,2,4-triazole or 1,3,4-thiadiazole)-methylthio-derivatives of quinazolin-4(3H)-one as DHFR inhibitors, Bioorg. Chem. 72 (2017) 282–292.
[42] H.-L. Qin, J. Leng, C.-P. Zhang, I. Jantan, M.W. Amjad, M. Sher, M. Naeem-ul-Hassan, M.A. Hussain, S.N.A. Bukhari, Synthesis of α, β-Unsaturated Carbonyl-Based Compounds, Oxime and Oxime Ether Analogs as Potential Anticancer Agents

for Overcoming Cancer Multidrug Resistance by Modulation of Efflux Pumps in Tumor Cells, J. Med. Chem. 59 (7) (2016) 3549–3561.
[43] N.A. Qandeel, A.K. El-Damasy, M.H. Sharawy, S.M. Bayomi, N.S. El-Gohary, Synthesis, in vivo anti-inflammatory, COX-1/COX-2 and 5-LOX inhibitory activities of new 2,3,4-trisubstituted thiophene derivatives, Bioorg. Chem. 102 (2020), 103890.
[44] S.T. Al-Rashood, G.S. Hassan, S.M. El-Messery, M.N. Nagi, E.E. Habib, F.A.M. Al-Omary, H.I. El-Subbagh, Synthesis, biological evaluation and molecular modeling study of 2-(1,3,4-thiadiazolyl-thio and 4-methyl-thiazolyl-thio)-quinazolin-4-ones as a new class of DHFR inhibitors, Bioorg. Med. Chem. Lett. 24 (18) (2014) 4557–4567.
[45] C.A. Lipinski, F. Lombardo, B.W. Dominy, P.J. Feeney, Experimental and computational approaches to estimate solubility and permeability in drug discovery and development settings, Adv. Drug Deliv. Rev. 46 (1–3) (2001) 3–26.
[46] D.F. Veber, S.R. Johnson, H.Y. Cheng, B.R. Smith, K.W. Ward, K.D. Kopple, Molecular properties that influence the oral bioavailability of drug candidates, J. Med. Chem. 45 (12) (2002) 2615–2623.
[47] R. Wang, Y. Fu, L. Lai, A new atom-additive method for calculating partition coefficients, J. Chem. Inf. Comput. Sci. 37 (3) (1997) 615–621.
[48] P.F. Lamie, J.N. Philoppes, 2-Thiopyrimidine/chalcone hybrids: design, synthesis, ADMET prediction, and anticancer evaluation as STAT3/STAT5a inhibitors, J. Enzyme Inhib. Med. Chem. 35 (2020) 864–879.
[49] M. Rbaa, S. Jabli, Y. Lakhrissi, M. Ouhssine, F. Almalki, T. Ben Hadda, S. Messgo-Moumene, A. Zarrouk, B. Lakhrissi, Synthesis, antibacterial properties and bioinformatics computational analyses of novel 8-hydroxyquinoline derivatives, Heliyon 5 (10) (2019) e02689, https://doi.org/10.1016/j.heliyon.2019.e02689.
[50] A. Radman Kastelic, R. Odzak, I. Pezdirc, K. Sovic, T. Hrenar, A. Cipak Gasparovic, M. Skocibusic, I. Primozic, New and Potent Quinuclidine-Based Antimicrobial Agents, Molecules 24 (14) (2019) 2675, https://doi.org/10.3390/molecules24142675.
[51] X. Jiang, W. Liu, W. Zhang, F. Jiang, Z. Gao, H. Zhuang, L. Fu, Synthesis and antimicrobial evaluation of new benzofuran derivatives, Eur. J. Med. Chem. 46 (8) (2011) 3526–3530.
[52] M. Durcik, P. Tammela, M. Barančoková, T. Tomašič, J. Ilaš, D. Kikelj, N. Zidar, Synthesis and Evaluation of N-Phenylpyrrolamides as DNA Gyrase B Inhibitors, ChemMedChem 13 (2018) 186–198.